N91-12405

6. ACCELERATION EFFECTS OBSERVED IN OPTICAL DATA TAKEN IN SPACELAB 3 FES

James Trolinger, SPECTRON Development Labs, Inc.
Ravindra Lal, Alabama A&M University
Rudy Ruff, NASA/Marshall Space Flight Center

ABSTRACT

Optical instrumentation in the Fluids Experiment System (FES) is briefly decribed. Samples of the data produced by the schlieren and holography systems during the Spacelab 3 flight are then presented with some of the holographic interferometry data being presented for the first time. Acceleration effects that can be observed in these data are discussed and the potential for using them as a basis for measurement is explored. This includes the tracking of deliberately introduced tracer particles and density gradients in the FES, the analysis of the existing concentration gradients, and a new fiber optic G-meter concept. Finally, some of the plans for acceleration measurement in the upcomng IML-1/FES are described.

I am going to describe some of the data from the Spacelab 3 flights that are relevant to this meeting. Dr. Lal of Alabama A&M University was the principal investigator and Rudy Ruff of NASA/Marshall Space Flight Center helped me put this presentation together. Figure 1 is a summary of the things I want to talk about, with particular attention given to some of the effects that are caused by residual acceleration. It also seems relevant to mention a particular additional acceleration instrument that we have been developing, and to mention some of the plans for the International Microgravity Laboratory (IML) experiments for measuring acceleration in the Fluids Experiment System.

SUMMARY

* FES OPTICAL INSTRUMENTATION
* SPACELAB 3 OPTICAL DATA
* OBSERVED EFFECTS OF ACCELERATION IN SPACELAB 3
* SOME IDEAS MAKING USE OF THE OBSERVED EFFECTS
* PLANS FOR IML-1/FES ACCELERATION MEASUREMENTS

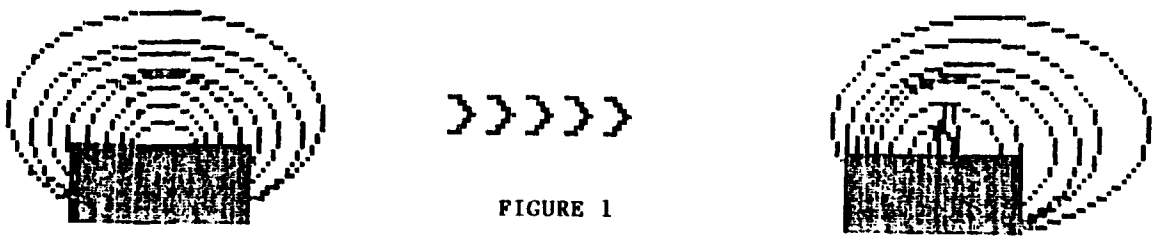

FIGURE 1

The optical instrumentation is summarized in Figure 2. It includes a Schlieren system, which observes the refractive index gradients while the crystal is growing in a diffusion-dominated field. The region around the crystal is depleted of solute which changes the refractive index. Therefore, instruments that measure refractive index will show this region around the crystal. You can also observe shadows or diffraction patterns of other things that may be in the flow field. I will show some examples of free-floating crystals that depict this. One nice thing about the Schlieren system is that it is a real-time system; you can observe by downlink on the closed-circuit TV while the experiment is operating.

The other system I'll discuss is the holographic system. It records holograms of the flow fields around the crystal from two different angles. In this system, there is a complete three-dimensional picture of any solids or materials that are moving around the crystal so that one has a quantitative measure of density, or refractive index, and ultimately the concentration of the solute surrounding the crystal.

For the Schlieren system, Figure 3, a helium-neon laser beam is expanded and collimated. The laser is located immediately above the crystal. A collimated beam of light travels across the crystal and is focused by a parabolic mirror before it crosses the knife edge and enters the vidicon camera.

Woven into this same optics are actually two holographic systems. The one shown in Figure 4 beams directly across the crystal, through the test cell,; onto the primary hologram film. Along the optical train, a beam is split off and that beam is mixed to provide a reference wave for the hologram. When this hologram is reconstructed, it is reilluminated with this reference wave and the full three-dimensional field and the restored wavefront are reconstructed from the hologram. Diagnostics can be applied to that reconstructed wavefront just as they could to the original wavefront.

C-2

FES OPTICAL INSTRUMENTATION

* SCHLIEREN SYSTEM OBSERVABLES
  - *REFRACTIVE INDEX GRADIENTS
  - *SOLID MATERIALS OF SUFFICIENT SIZE (DIFFRACTION PATTERN)
  - *OBSERVED ON CCTV IN REAL TIME

* HOLOCAMERA
  - *REFRACTIVE INDEX
  - *SOLID MATERIALS (3-D IMAGE)
  - *OBSERVED WITH HOLOGRAMS AT A LATER TIME

FIGURE 2

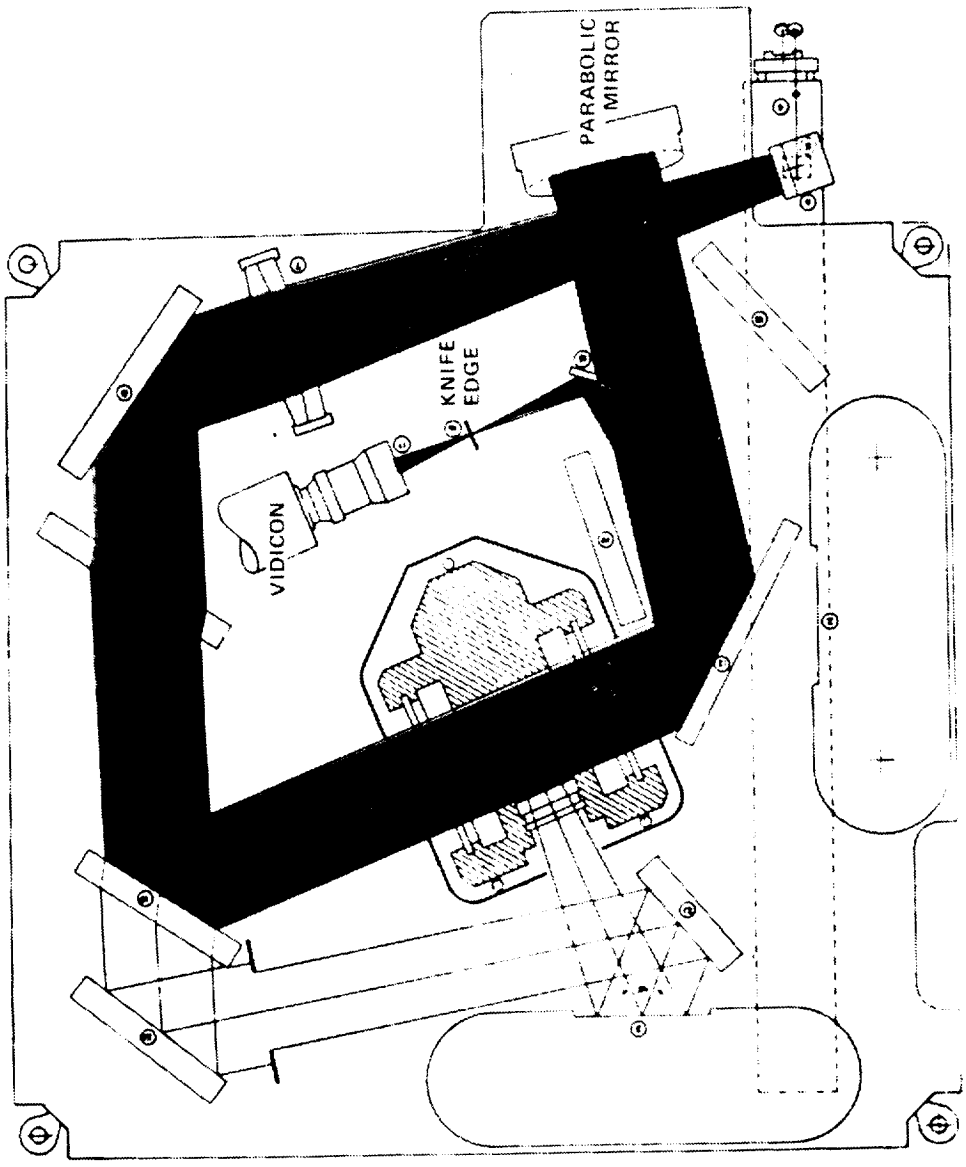

FIGURE 3.

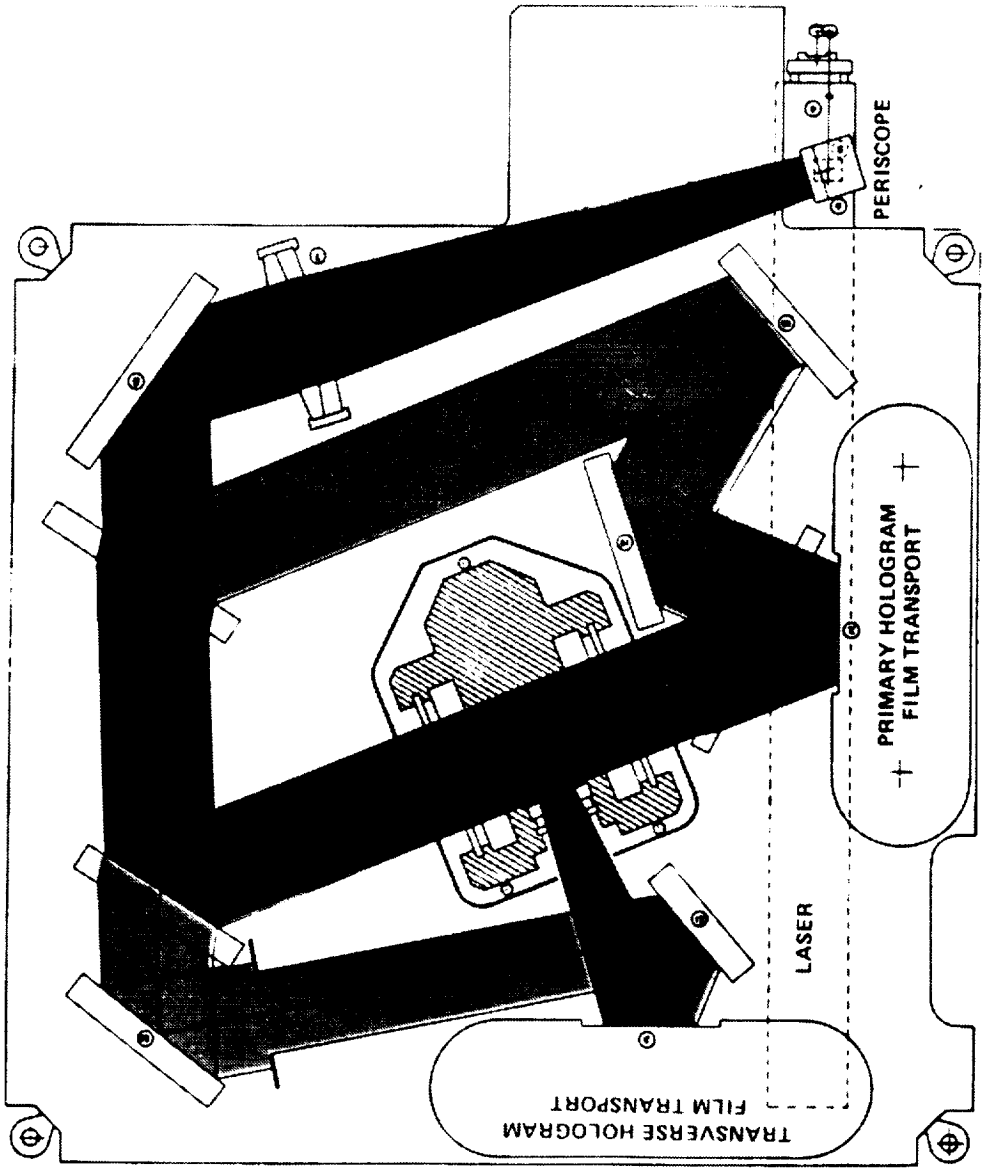
PERISCOPE
PRIMARY HOLOGRAM
FILM TRANSPORT
LASER
TRANSVERSE HOLOGRAM
FILM TRANSPORT

FIGURE 4.

These holograms are generated almost continuously during the experiment after the cap is removed from the crystal and growth has started. These holograms were generated every few seconds. The holographic data disadvantage is that it cannot be examined until the mission is over. This was the first time holograms have been made in space and we were not sure that the system would produce good holograms in space, because of a number of considerations that were not possible to test in the earth's environment.

Figure 5 summarizes the observations made with the holographic system. The system worked almost flawlessly for the entire flight, with hundreds of holograms and many hours of video tapes made. There are tremendous amounts of data which we are just beginning to analyze. A bonus that was not expected was the observation of free-floating crystals. These crystals could also be used for measurements. Refractive index changes and the effects of accelerations on these were observed. The concentration and, consequently, the refractive index around the crystal should be symmetrical and uniform for proper crystal growth. Acceleration was observed to push this back and forth and make the concentration nonsymmetrical. In some cases, impulses, dumps, or large motions (accelerations) were indicated by the crystals making large movements in short periods of time.

The crystal is shown in Figure 6, and the rays of light pass through the zone of concentration gradients. As the concentration increases, as during crystal dissolution, the rays will be bent toward the increasing refractive index. As the crystal grows, the region immediately surrounding it is depleted, and the refractive index decreases, so that the light ray coming through that zone gets blocked. The closed-circuit television camera shows a picture of the crystal and the surrounding zone of different concentration.

The lower portion of Figure 6 shows the effects of acceleration on the differing concentration region. During null acceleration, you see a more or less symmetrical dark region. The figure on the right shows the rays that have been bent and moved out of the field. A free-

OBSERVATIONS

* SUSPENDED CRYSTAL MOTION (FLOATERS)
* REFRACTIVE INDEX FIELD CHANGES
* UNSYMMETRICAL REFRACTIVE INDEX FIELD
* CONVECTIVE MOTION PERSISTING FOR HOURS
* IMPULSES EASILY OBSERVED
* MICROGRAVITY AND SMALL VARIATIONS MORE DIFFICULT

FIGURE 5

SPACELAB 3 OPTICAL DATA- SCHLIEREN

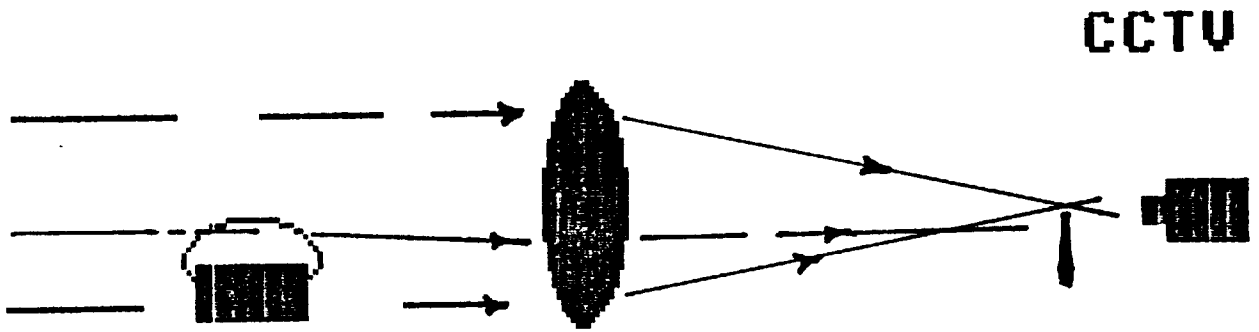

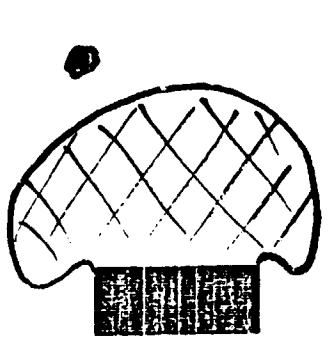

NO ACCELERATION

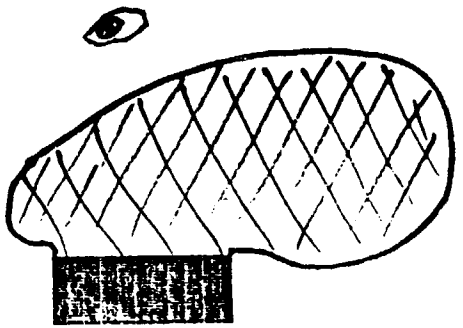

ACCELERATION

FIGURE 6

floating particle would be similar. It would be a small spherical blob that is surrounded by a dark region because a free-floating crystal is also growing. Under acceleration one may observe quite drastic movement of the plume off to one side, and the free-floating crystal would move with the appearance of a comet. It would drag the region of lower refractive index at a different velocity.

Figure 7 shows an actual picture from the closed-circuit TV screen. You are looking through the cell and can see the crystal and the plume. This was early in the experiment, when the acceleration was low and significant acceleration effects are not observed. Later, it becomes extremely difficult to analyze the data quantitatively. One must make some assumptions about symmetry. Once the field moves to the side, it becomes impossible to know what the symmetry is, the data cannot be analyzed in a quantitative sense.

A similar effect for the holographic interferometry is shown in Figure 8. There were several types of holographic recordings done. The passage of the light beam is again delayed over the crystal and the wavefront is phase-shifted as it passes through the region of different refractive indices. This information is stored on the hologram. The standard interferometry technique is to reconstruct just the starting wave, and mix it with an interferometer reference wave, which gives an inteferogram. For the null-acceleration case, the interferogram has field lines that look symmetrical, and the free-floating crystal is surrounded by a circular set of fringes. At the onset of acceleration, these fringes push off to the side. This can be viewed as a buoyant force pushing the bubble in the opposite direction of the acceleration.

Figures 9 and 10, were made by Bill Witherow of NASA and I think Bob Naumann used a similar set to calculate the g forces taking place as the particle moved. These are double exposure holographic interferograms, and there are a number of things to see in these figures. You can see a free-floating crystal that is sitting on the corner of the TGS crystal, which is no longer a cylinder. It has taken a different shape now. Five hours later the crystal has moved, and two hours after that it has moved even more. Ultimately, it moved out of the field of view.

FIGURE 7.

SPACELAB 3 OPTICAL DATA- HOLOGRAPHY

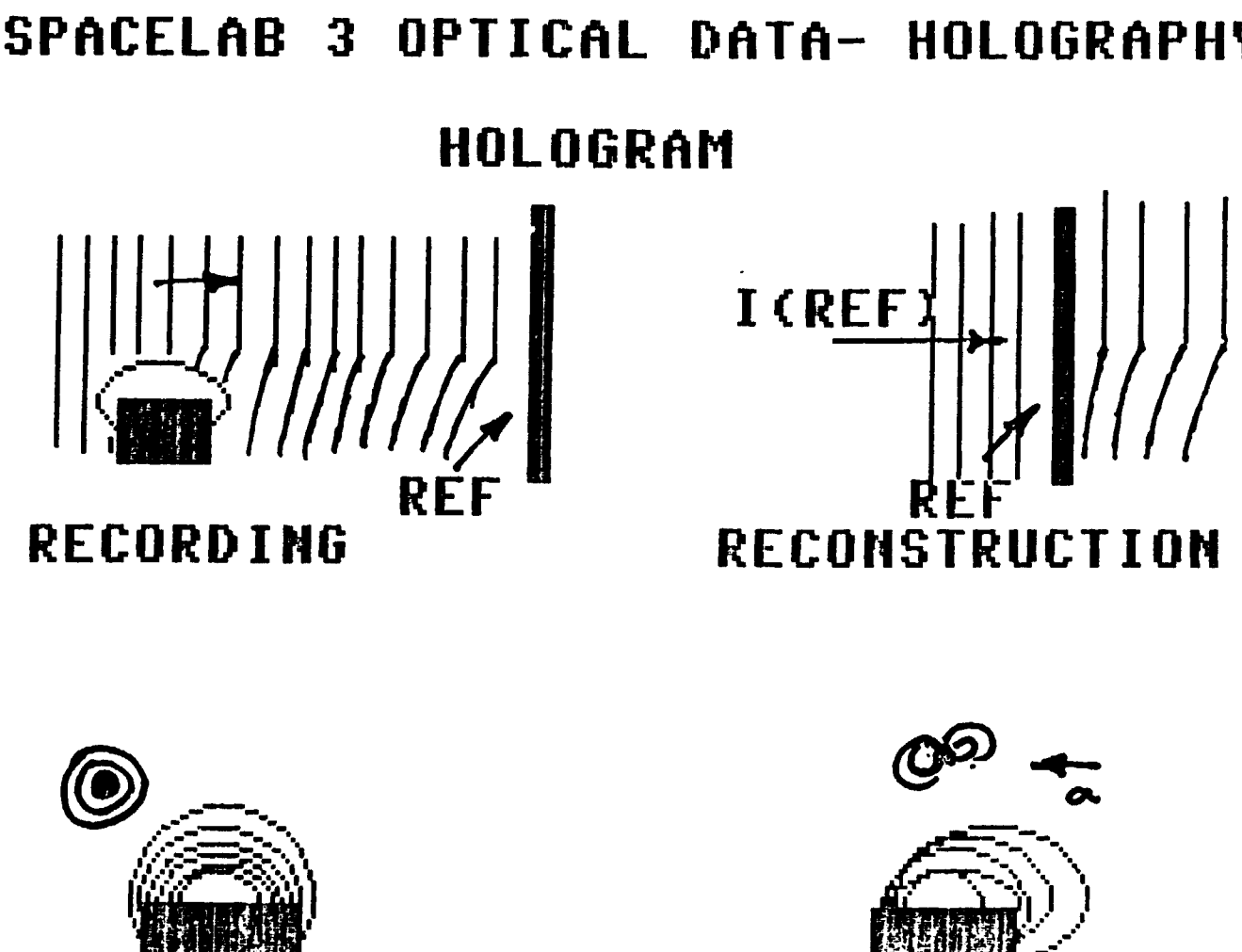

FIGURE 8

BLACK AND WHITE PHOTOGRAPH

DOUBLE EXPOSURE HOLOGRAMS
(FES CELL 203)
SL3

FIGURE 9.

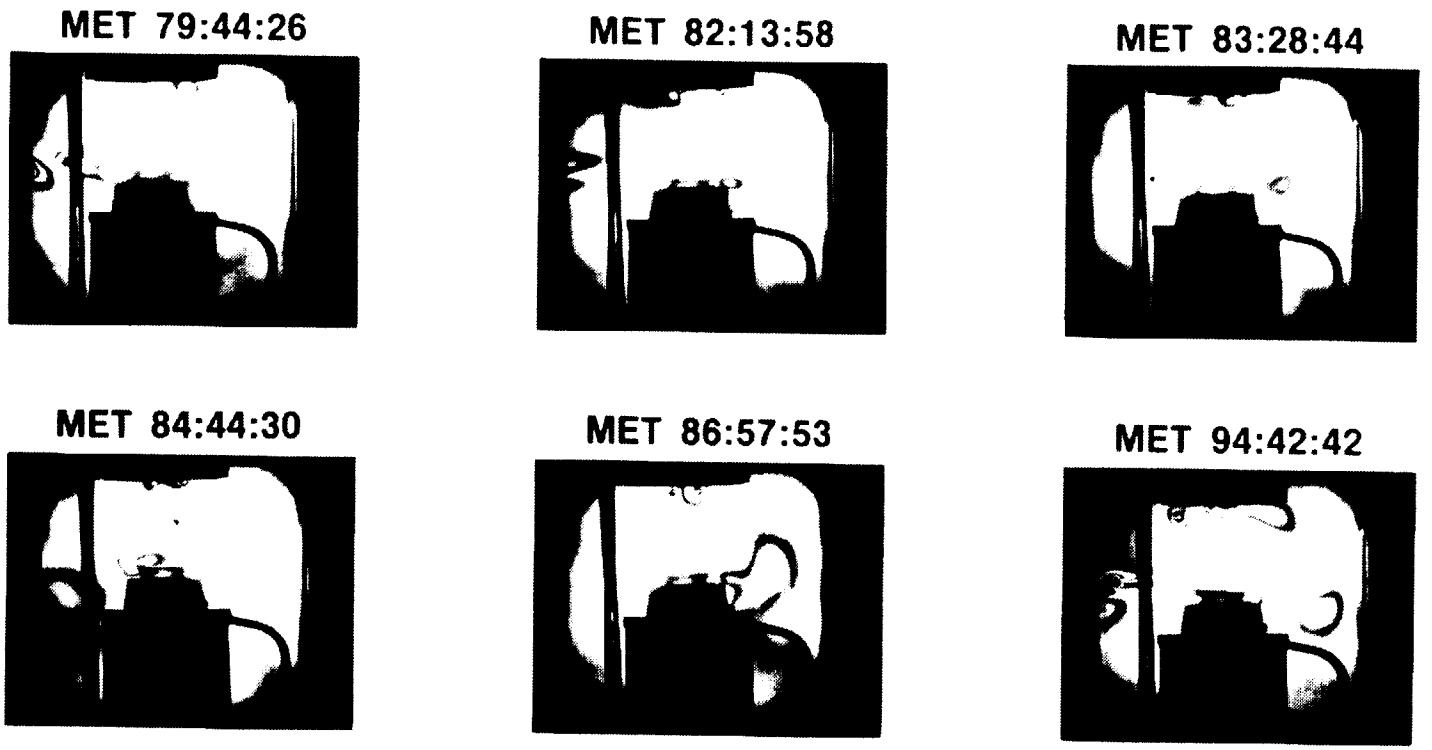

DOUBLE EXPOSURE HOLOGRAMS
(FES CELL 203)
SL3

FIGURE 10.

The crystal is moving extremely small amounts during the time between two exposures. You cannot really see motion of the crystal itself, but you can see the region around it because the change in the concentration produced a set of fringes. There was virtually no change in the crystal itself between these two times, or in the concentration around the crystal, so you see no fringes on some of the figures. In other cases, there is a small change but definitely a concentration gradient change between the two exposures.

I have summarized the consequences of what was seen in Figure 11. The FES experiment is not particularly interested in acceleration, but in convective flow, whether the process is diffusion-controlled or not. There is obviously convective flow that is being measured by several things. This flow will lead to a non-uniform concentration, but the question is: how much? That is yet to be analyzed and modeled, and is presently being done. This potentially would lead to a non-uniform growth. A side effect is that it makes the experiment and analytical calculations difficult, but we have developed an alternate solution.

We have looked at some ideas for measuring acceleration in Figure 12, more specifically, convective flow in the FES. It was a bit of serendipity that the free-floating crystal could be used to measure acceleration. We are considering deliberate seeding of the FES and that will probably be done in the IML-1 experiment. There is a potential problem if you put particles into the flow, in that one of those particles will certainly wind up where it is not wanted. So it would be nice if one could put a dissipative seeding that would not reach the crystal. We considered the possibility of stretching a wire with exposed centers across the fluid, so one could actually add a temperature change, or density gradient, into the flow. One could then add tracer refractive index gradients anywhere in the fluid that could be traced with the Schlieren and the holography systems. Dr. Lal and his team are considering modeling the plume by adding acceleration as a parameter. He and Dr. Wilcox have created a general model for the crystal growth. It can predict what the density gradients or the concentration gradients will be, but it could include acceleration for ultimate use as a measurement tool.

CONSEQUENCES

* CONVECTIVE FLOW OVER CRYSTAL
* NON UNIFORM CONCENTRATION
* NON UNIFORM GROWTH
* ERROR IN ABEL INVERSION OF DATA

FIGURE 11

IDEAS FOR ACCELERATION MEASUREMENT

* ADD TRACER PARTICLES-MONITOR MOTION
* ADD TRACER REFRACTIVE INDEX CENTERS
* MODEL EXISTING PLUME RE ACCELERATION
* FIBER OPTIC G SENSOR

FIGURE 12

Bubble mechanics is a subject that has not been treated much in zero g. Think, in the general sense, of a bubble which is a density of one value, within a density of another value, as shown in Figure 13. I have separated this into three effects; acceleration, diffusion, and density. If there is no acceleration, then is there is a diffusion of one density into the other. In this case, there is a diffusion layer that looks like the second picture. So, this bubble essentially grows. In the G-field, the bubble does two things. The center of gravity will move, but the bubble will not hold its shape because of viscous forces and drag. It will be distorted. The bubble in the acceleration field will change shape due to a combination of these effects as shown at the bottom of the figure. Those two effects must be separated in order to use this as a measure. That is a reason to want very small bubbles in the flow field -- their center of gravity would be easier to locate. The distortion effects of the bubble would not play a big role.

We have developed a number of fiber optic sensors (Figure 14) to measure electric fields, magnetic fields, gravitational fields, and flow fields. Basically, the device injects a wave front into the fiber. One of the paths is a fixed leg of the Mach Zehnder interferometer and the other has the sensing element on it. In the case of measuring gravity, there is a mass on that element. Analysis of the phase differs between the two legs, leads to measurable function of acceleration. In the case of a flow field, the drag across the fiber stretches one leg of the Mach Zehnder interferometer. Appendix A shows the simple derived relationship. The longer the fiber, the more sensitive the accelerometer is, and the larger the mass the more sensitive it is. We have not yet demonstrated this for gravitational fields, but we have demonstrated it for electric and magnetic fields. Putting numbers into this equation for some practical geometries, fiber types, and measurement of phase, shows that nano-g sensitivity is achievable.

Figure 15 is a summary of some of IML-1 plans that make use of things that we have learned from Spacelab 3. The IML will seed the flow field, probably with polystyrene spheres, and track the motion to measure acceleration or to measure convective flow. Because of the problem

DENSITY GRADIENT IN A G FIELD

-BUBBLE MECHANICS-

ZERO-G DIFFUSION-DISTORTION-CG MOTION

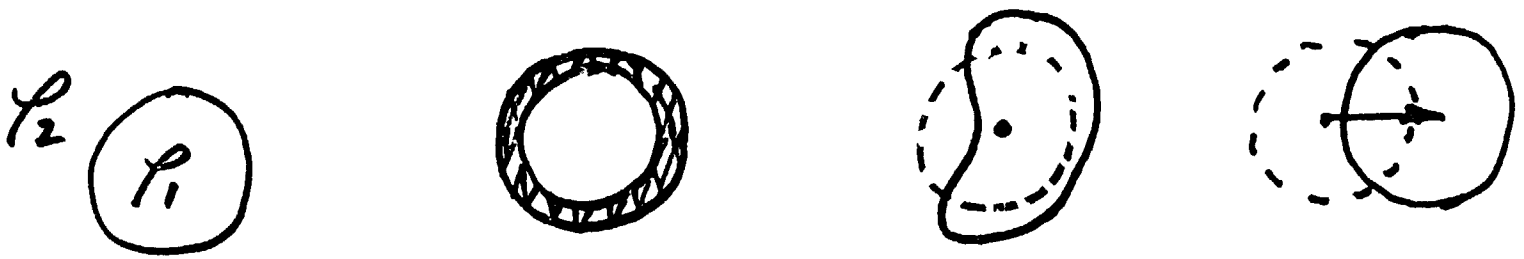

COMBINATION OF ABOVE

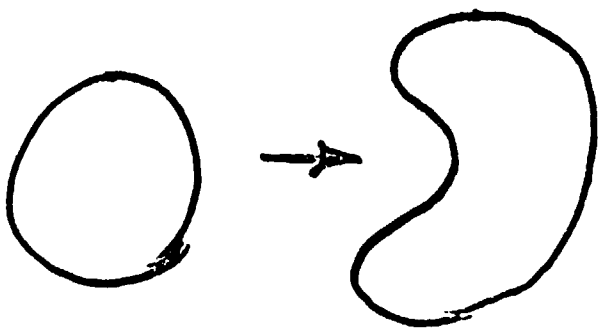

FIGURE 13

FIBER OPTIC G-SENSOR

* OPTICAL FIBER STRETCHED ACROSS FLUID
* FIBER LENGTH OR POSITION CHANGED BY ACCELERATION
* FIBER SENSOR IS ONE BRANCH OF A MICHELSON INTERFEROMETER
* ATTAINABLE SENSITIVITY 10^{-9} G

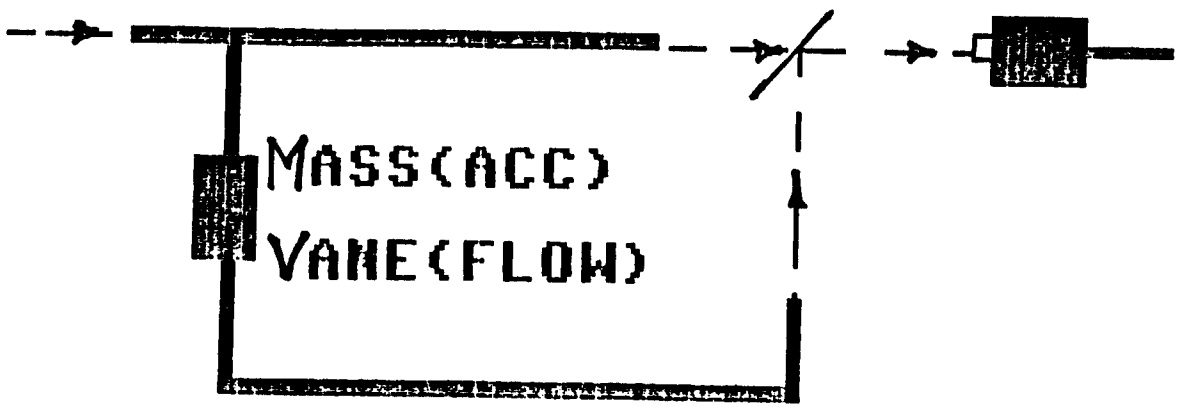

FIGURE 14

IML-1 PLANS

* SEED FES WITH POLYSTYRENE SPHERES
* TRACK SPHERE MOTION
* THREE VIEWING ANGLES
* MEASURE CONVECTIVE FLOW

HOE

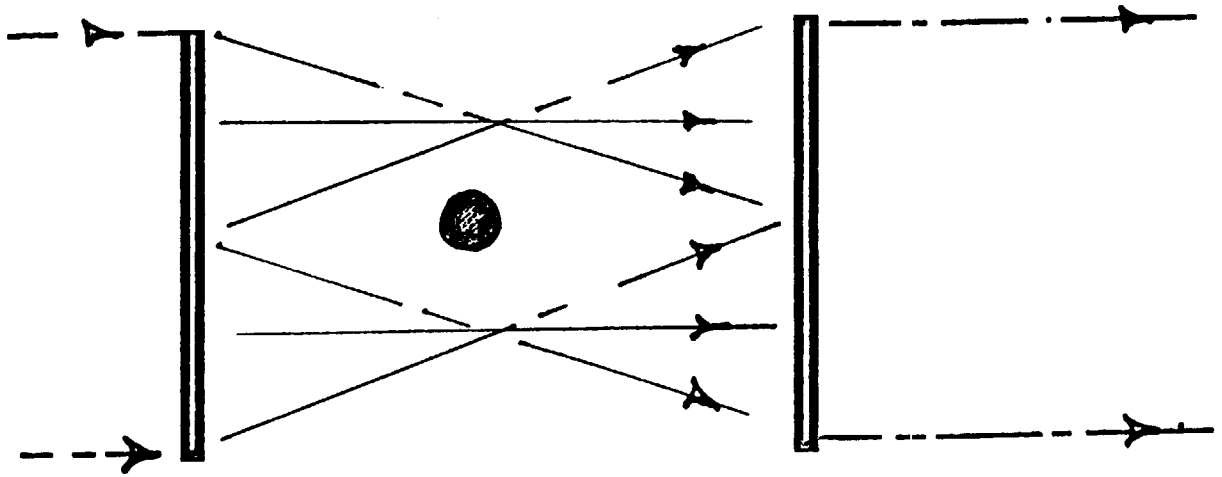

FIGURE 15

that is now known as non axi-symmetry in the growth field, there are plans to look across the crystal at a number of angles so that this can be compensated. We have tomography equations that are reasonably accurate for views across the crystal at ± 15 degrees, providing a full three-dimensional density distribution.

We will use a holographic element on one side of the crystal to split the beam into three beams across the crystal and another one on the opposite side to recombine the beams. This will also help to track particles in three dimensions, and it will give a higher resolution.

Ken Demel, NASA/Johnson Space Center: Do you have any quantitative correlations between displacements and accelerations?

Trolinger: As far as I know the only calculations that yield hard numbers on gravity are those by Bob Naumann. We haven't actually modeled the flow field or any of the density gradients to try to do this yet.

John Williams, the Center for Space and Defense Technology: Early in the FES program we talked in terms of a performance parameter on being able to detect the change in index of refraction of 10^{-5} or so. Do you have a feel for where we stand now as far as detection sensitivity?

Trolinger: I think we met all of those specifications. Among others, I was surprised at how well the system really worked. The holography system and holographic interferometry system was extremely rewarding in how well the data is coming out. There are some problems here and there, but basically I think most of the specifications of the original design were met.

Lodewijk van den Berg, EG&G: I have a flippant answer to that but it's of course due to the extreme care taken by the people that were operating the equipment (Dr. van den Berg was the payload specialist for this experiment). In all these extraneous motions that you saw in the solution, is it possible to track those motions in the quality of the crystal that was obtained? In other words can you see the dif-

ferent regions in the crystal that are damaged by these motions or is the crystal just homogeneous throughout, in other words, this kind of much lower than 1-g motions, did it have an effect on the crystal?

Trolinger: I will call on Ravi Lal to answer since he has the crystal.

Lal: We cannot, at the present time, correlate the motions observed in the solution due to the disturbances with the defects in the grown crystal. However, we have found different amounts of growth at different locations of the seed. This is an anomaly and can only be attributed to time-periodic growth rate.

Question: Did you take the motion of the free-floating crystal around the fixed crystal to calculate the local gravity gradient?

Trolinger: The question was were we assuming the gravity gradient background to calculate the motion of the particle. Bob Naumann's answer is yes.

Bob Naumann, NASA/Marshall Space Flight Center: I'm not quite sure that the calculations agree properly. We still have work to do on that.

Byron Lichtenberg; Payload Systems, Inc: Could the free-floating crystals explain the distorted concentration?

Trolinger: The data shown for the free-floating crystal was from one cell. The third cell, from which the interferometry data was shown, actually did not have any free-floating crystals, so you really couldn't explain that with distortion. There would be some distortion, certainly, by the free-floating crystal. Also those free-floating crystals were only present during a small part of the mission. Ultimately a larger acceleration would scoot those things off to the side and they would be completely out of the field of view. Also there were some actual correlations, especially with the water dump near the end of the mission. That was postponed as long as possible. The plume was sitting there, and when that occurred, it just swooshed over. So accelerations were actually correlated with some of the gradients in concentration.

APPENDIX A

A SENSITIVE FIBER-OPTIC ACCELEROMETER

K. A. Arunkumar
Spectron Development Laboratories, Inc.
3303 Harbor Blvd., Suite G-3
Costa Mesa, California 92626
(714) 549-8477

Abstract

A sensitive fiber-optic accelerometer which can measure accelerations down to nano-g's has been proposed.

The Proposed Accelerometer

Fiber-optic interferometric accelerometer with μg sensitivity has been demonstrated by Tveten.[1] In this communication, we propose a simple method to improve its sensitivity by at least a couple orders of magnitude. The accelerometer in reference 1 employs axial stretching of one of the arms of an all fiber Mach-Zehnder and the measured phase difference $\delta\phi$ is related to the acceleration by

$$\text{Acceleration } a = \frac{\lambda r^2 Y}{2m2L}\,\delta\phi \qquad (1)$$

where r, 2L and Y are the radius, length, and Young's modulus of the fiber, respectively, and m is the mass undergoing acceleration.

Accelerations can also be measured when the moving mass bows one arm of the interferometer instead of stretching it axially (transverse accelerometer), see Figure 1.

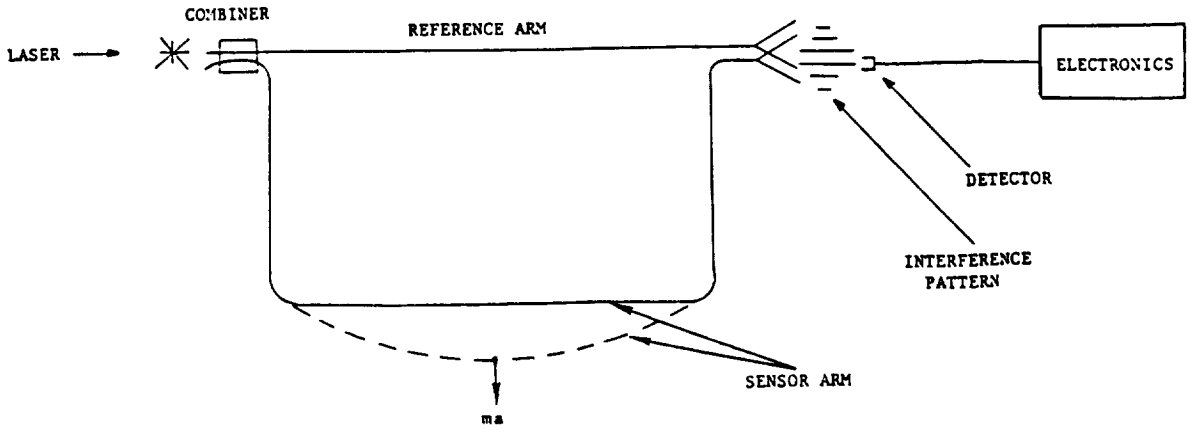

Fig. 1. Schematic of the Proposed Accelerometer

KAA-26/19

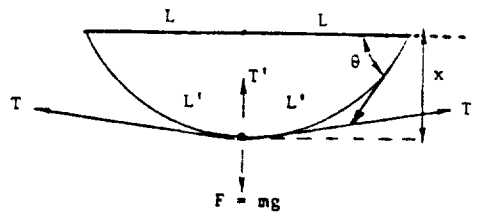

Figure 2. Fiber Bowing When Subjected to Acceleration

Analysis

For small displacement y, the phase difference

$$\delta\phi = \frac{4\pi}{\lambda}\left[\sqrt{x^2 + L^2} - L\right] \text{ and } x = \left(\frac{L\lambda}{2\pi}\right)^{1/2} \delta\phi^{1/2}$$

Under equilibrium conditions, $F = T' = 2T \sin\theta$ where T is the tension in the fiber. Using the definition for Young's modulus, $\delta\phi$ can also be expressed as

$$\delta\phi = \frac{2\pi}{\lambda}\frac{2L}{Y}\frac{T}{\pi r^2}$$

Combining the above relations, we have for the phase difference

$$\delta\phi = \frac{2\pi}{\lambda}\frac{2L}{Y}\frac{F}{2x}\frac{\sqrt{x^2 + L^2}}{\pi r^2} \quad \text{and for}$$

acceleration

$$a = \left(\frac{\lambda}{2\pi L}\right)^{3/2} \cdot \frac{Y}{m} \cdot \pi r^2 \cdot (\delta\phi)^{3/2} \tag{2}$$

where it is assumed that $L \approx L'$ for $y \ll L$.

Discussion

A 10 kg mass undergoing 9.8×10^{-6} m/sec^2 (μg) acceleration can cause a $\delta\phi \sim 1.4 \times 10^3$ rad when a fiber of active length 1m and r = 2μ is stretched longitudinally (axial accelerometer). Under the same condition, transverse stretching (bowing) results in a phase shift of 1.36×10^4, an order of magnitude greater than the former. This property of the latter will be helpful while measuring ng (nano-g) accelerations.

Under ng acceleration, the axial accelerometer will produce a phase shift of 1.414 rad whereas the transverse accelerometer will induce a $\delta\phi$ of 135.6 radians. The phase change detection technique for the latter can be much simpler than that to be used for the former. Moreover, acceleration measurement using the fiber bowing technique can greatly simplify the experimental setup.

Reference

A. B. Tveten, A. Dandridge, C. M. Davis, and T. G. Giallorenzi, Electron. Lett., Vol. 16, pp. 854-855, 1980.